Available online at www.sciencedirect.com
ScienceDirect
Trans. Nonferrous Met. Soc. China 31(2021) 2651−2663
Transactions of Nonferrous Metals Society of China
www.tnmsc.cn

Effect of heat treatment on mechanical and wear properties of Zn−40Al−2Cu−2Si alloy

Temel SAVAŞKAN[1], Zeki AZAKLI[2], Ali Paşa HEKİMOĞLU[3]

1. Mechanical Engineering Department, Haliç University, 34445, İstanbul, Turkey;
2. Mechanical Engineering Department, Gümüşhane University, 29010, Gümüşhane, Turkey;
3. Mechanical Engineering Department, Recep Tayyip Erdogan University, 53100, Rize, Turkey

Received 2 November 2020; accepted 18 April 2021

Abstract: In order to determine the effect of heat treatment on the mechanical and wear properties of Zn−40Al−2Cu−2Si alloy, different heat treatments including homogenization followed by air-cooling (H1), homogenization followed by furnace-cooling (H2), stabilization (T5) and quench−aging (T6 and T7) were applied. The effects of these heat treatments on the mechanical and tribological properties of the alloy were studied by metallography and, mechanical and wear tests in comparison with SAE 65 bronze. The wear tests were performed using a block on cylinder type test apparatus. The hardness, tensile strength and compressive strength of the alloy increase by the application of H1 and T6 heat treatments, and all the heat treatments except T6, increase its elongation to fracture. H1, T5 and T6 heat treatments cause a reduction in friction coefficient and wear volume of the alloy. However, this alloy exhibits the lowest friction coefficient and wear volume after T6 heat treatment. Therefore, T6 heat treatment appears to be the best process for the lubricated tribological applications of this alloy at a pressure of 14 MPa. However, Zn−40Al−2Cu−2Si alloy in the as-cast and heat-treated conditions shows lower wear loss or higher wear resistance than the bronze.
Key words: Zn−Al based alloys; heat treatment; structural features; mechanical properties; lubricated friction and wear

1 Introduction

Zinc−aluminum based alloys have attracted the attention of the researchers working on the development of bearing alloys due to their multi-phase microstructures consisting of soft and hard phases that facilitate sliding and load bearing, and high specific strength [1−4]. Extensive research on the microstructure and properties of these alloys has resulted in the development of a number of Zn−Al based bearing alloys containing small amount of alloying additions including copper, silicon and magnesium [5−7]. These studies have shown that the hardness, strength and wear resistance of Zn−Al alloys increase to a certain extent with the addition of alloying elements [5−7]. The increase in the wear resistance of the Zn−Al based alloys was attributed to the increase in their hardness and strength [8,9].

Copper and/or silicon containing monotectoid Zn−Al based alloys were shown to have superior mechanical and tribological properties compared to the eutectic and eutectoid alloys [9−12]. It is known that copper additions improve the mechanical properties of Zn−Al alloys due to solid solution hardening and the formation of relatively hard intermetallic ε ($CuZn_4$) and T' (Al_5Zn_4Cu) phases [5]. Metastable ε phase is formed in Zn−Al alloys containing more than a certain amount of copper (usually 2%) depending on their zinc content. Formation of T' phase results from decomposition of ε phase by a four-phase reaction of $\alpha+\varepsilon\rightarrow T'+\eta$ [13]. Silicon additions also increase

Corresponding author: Ali Paşa HEKİMOĞLU, Tel: +90-464-223-54-81, E-mail: ali.hekimoglu@erdogan.edu.tr
DOI: 10.1016/S1003-6326(21)65682-0

the hardness and strength of both binary Zn−Al and ternary Zn−Al−Cu alloys to a certain extent, and provide load-bearing ability in bearing applications [6,9,14]. However, when the copper or silicon content of Zn−40Al based alloys exceeds 2%, the tensile strength and wear resistance of these alloys decrease. This decrease results from the formation of relatively hard and brittle ε ($CuZn_4$) phase and the change in the size and distribution of silicon particles. It is known that when the copper and silicon contents exceed 2%, the size and volume fraction of both ε phase and silicon particles increase and their distribution becomes inhomogeneous [11,12]. This results in a decrease in the tensile strength and wear resistance of the ternary and quaternary alloys by causing brittleness [5,6,8]. Significant effects of these alloying elements on the mechanical properties and wear resistance of Zn−Al alloys have led to the development of ternary Zn−40Al−2Cu and quaternary Zn−40Al−2Cu−2Si alloys [9,11,12]. The quaternary Zn−40Al−2Cu−2Si alloy exhibited the highest hardness, strength and wear resistance among the ones developed [12]. This was attributed to the microstructure and mechanical properties of this alloy [12]. It is also known that the physical stability and mechanical properties of these alloys can be improved by the application of suitable heat treatments [13,15,16]. These heat treatments were performed by homogenization, stabilization and quench-ageing [13,15−17]. It is well known that homogenization is applied by heating the alloys up to a temperature close to the solidus temperature and keeping them at this temperature for a certain period of time. The reason for this treatment is to obtain chemical homogeneity and reduce micro segregation in the as-cast alloys by diffusion of atoms, and improve their machinability [18,19]. Stabilization is carried out by heating the alloys to a temperature above their working temperature but below the transformation temperature, followed by cooling to room temperature. The main reason for this heat treatment is to improve dimensional stability of the as-cast alloys [18,19]. Quench−aging is performed by solution treatment followed by rapid cooling (quenching) and aging of alloys to obtain the desired physical and mechanical properties [18,19]. The final microstructure and properties obtained after this treatment depends on the aging temperature and time [13,15,16,18,19]. However, the influence of different heat treatments on the structural, mechanical and tribological properties of the quaternary Zn−40Al−2Cu−2Si alloy has not been studied systematically. It was also observed that the tribological properties of this alloy have not been investigated at contact pressures above 6 MPa. However, the studies have shown that this alloy can be considered as an alternative material for the manufacture of diesel engine crankshaft journal bearings, which work under a pressure of approximately 14 MPa [20]. Therefore, the aim of this work is to study the effects of different heat treatments including stabilization, homogenization and quench−aging on the mechanical and tribological properties of Zn−40Al−2Cu−2Si alloy in comparison with SAE 65 bearing bronze and determine the most suitable heat treatment for its tribological applications at a pressure of 14 MPa.

2 Experimental

Zn−40Al−2Cu−2Si alloy was made by permanent mold casting method using high-purity (99.9%) zinc, commercially pure (99.7%) aluminum, and Al−50Cu and Al−12Si master alloys. Melting was carried out in an electric pot furnace. The molten alloy was poured at 680 °C to a conical-shaped steel mold having dimensions of 45 mm × 60 mm × 190 mm. SAE 65 bronze was purchased from a commercial source. The chemical composition of the alloys was determined using atomic absorption spectrometry (AAS) analysis. The alloy was subjected to different heat treatments. They were homogenization followed by air-cooing (H1), homogenization followed by furnace-cooling (H2), stabilization (T5) and quench−aging (T6 and T7) treatments. The conditions for these heat treatments are given in Table 1.

The as-cast and heat-treated samples of the alloy were prepared by standard metallography methods. They were etched with 20% nital (20% nitric acid + 80% ethyl alcohol) solution to reveal their microstructures. The microstructures of the metallographic samples were examined using a JEOL 6400 scanning electron microscope (SEM) equipped with an energy-dispersive X-ray spectrometer (EDS). In order to confirm the phases present in the microstructure of the alloy samples, X-ray diffraction (XRD) studies were conducted.

Table 1 Conditions of H1, H2, T5, T6 and T7 heat treatments

Treatment	Application conditions
H1	Homogenization at 375 °C for 36 h followed by air-cooling
H2	Homogenization at 375 °C for 36 h followed by furnace-cooling
T5	Artificial aging at 150 °C for 100 h
T6	Solutionizing at 375 °C for 36 h, and quenching and artificial aging at 180 °C for 2 min
T7	Solutionizing at 375 °C for 36 h, and quenching and artificial aging at 180 °C for 8 h

These studies were carried out on flat specimens at a scanning speed of 1 (°)/min using Cu K_α radiation. Densities of the samples of the alloy and the bronze were determined by dividing the measured mass values by the calculated volume values. A micrometer with a precision of 0.001 mm and a balance with an accuracy of 0.01 mg were used for length and mass measurements, respectively. Brinell hardness values of the samples were measured using a 2.5 mm diameter ball as an indenter under 62.5 kg load. The hardness of each sample was taken as the average of at least five measurements. Tensile and compression tests were carried out with the samples having the dimensions of *d*10 mm × 50 mm and *d*10 mm × 10 mm, respectively, at a deformation rate of 5×10^{-3} s^{-1}.

Tribological properties of the alloy were investigated in the as-cast and heat-treated conditions using a block on cylinder type test apparatus, the schematic diagram of which is shown in Fig. 1(a). This test apparatus simulates the contact between the shaft and the journal bearing in real applications. The construction details of this test machine have been given in the previously published works [10,11]. A close-up photograph of the wear test apparatus showing the type of contact between the wear sample and the cylinder is given in Fig. 1(b). The cylinder of the apparatus was made of SAE 4140 steel that was hardened and tempered to obtain a hardness of about 55 RSD-C. The surface roughness of the cylinder was kept below 1 μm by grinding and polishing operations. The technical drawing of the wear sample is shown in Fig. 2. The wear samples were weighed before

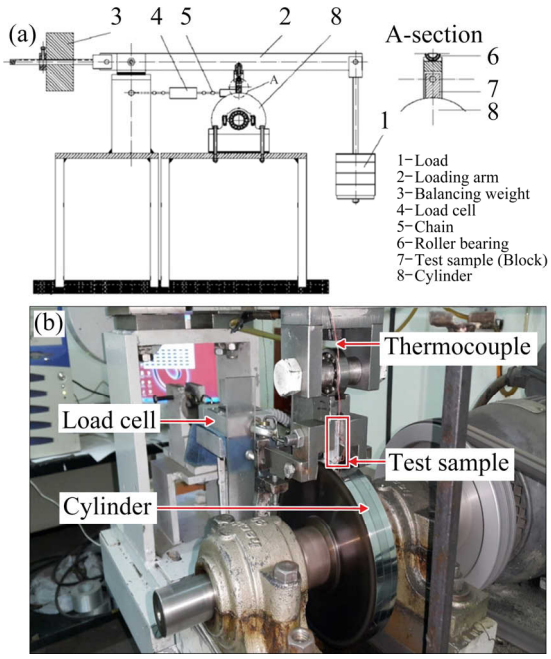

Fig. 1 Schematic illustration of wear test apparatus (a), and close-up view of apparatus showing contact between sample and cylinder (b)

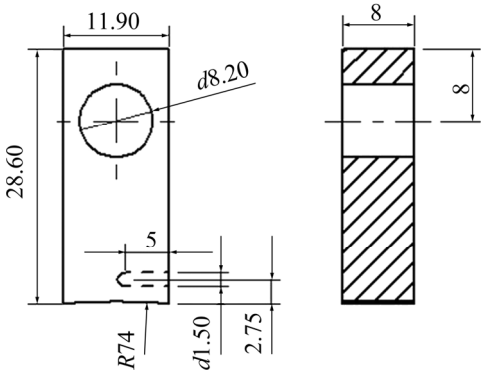

Fig. 2 Technical drawing of wear test sample (Unit: mm)

and after each test using a balance with an accuracy of 0.01 mg, following ultrasonic cleaning in appropriate chemical solvents. The volume loss due to wear was calculated by dividing the measured mass loss by the density of the alloy. The friction force was measured using a load cell. Voltage values obtained from the load cell were converted to friction force and friction coefficient by means of a software. The temperature of the wear samples was monitored during the tests with a copper−nickel type thermocouple placed in a hole drilled 2.75 mm above the contact surface. The wear tests were performed at an oil flow rate of 1 cm^3/h, a pressure of 14 MPa and a sliding speed of 2 m/s for a sliding distance of 102 km. SAE 20W/50 engine

oil was used for the tests. Surface roughness of the wear samples and the cylinder were measured with a measuring device (MAHR MarSurf M 300) before and after each test.

3 Results

3.1 Results of chemical analysis and metallography

Chemical compositions of Zn−40Al−2Cu−2Si alloy and SAE 65 bronze are given in Table 2.

Table 2 Chemical compositions of Zn−40Al−2Cu−2Si alloy and SAE 65 bronze

Material	Zn	Al	Cu	Si	Sn
Zn−40Al−2Cu−2Si alloy	56.3	39.9	1.9	1.9	−
SAE 65 bronze	−	−	88.3	−	11.7

The as-cast microstructure of Zn−40Al−2Cu−2Si alloy consisted of aluminum-rich α dendrites eutectoid $\alpha+\eta$ phase mixture, and copper-rich ε ($CuZn_4$) and silicon particles, as seen in Fig. 3(a). However, the ε particles were hardly observed in the microstructure of the alloy due to its low copper content. The microstructures produced by different heat treatments including homogenization (H1 and H2), stabilization (T5) and quench−aging (T6 and T7) are shown in Figs. 3(b−f), respectively. XRD patterns of the as-cast and heat-treated samples of Zn−40Al−2Cu−2Si alloy are shown in Fig. 4. It can be seen that these patterns confirm the presence of the

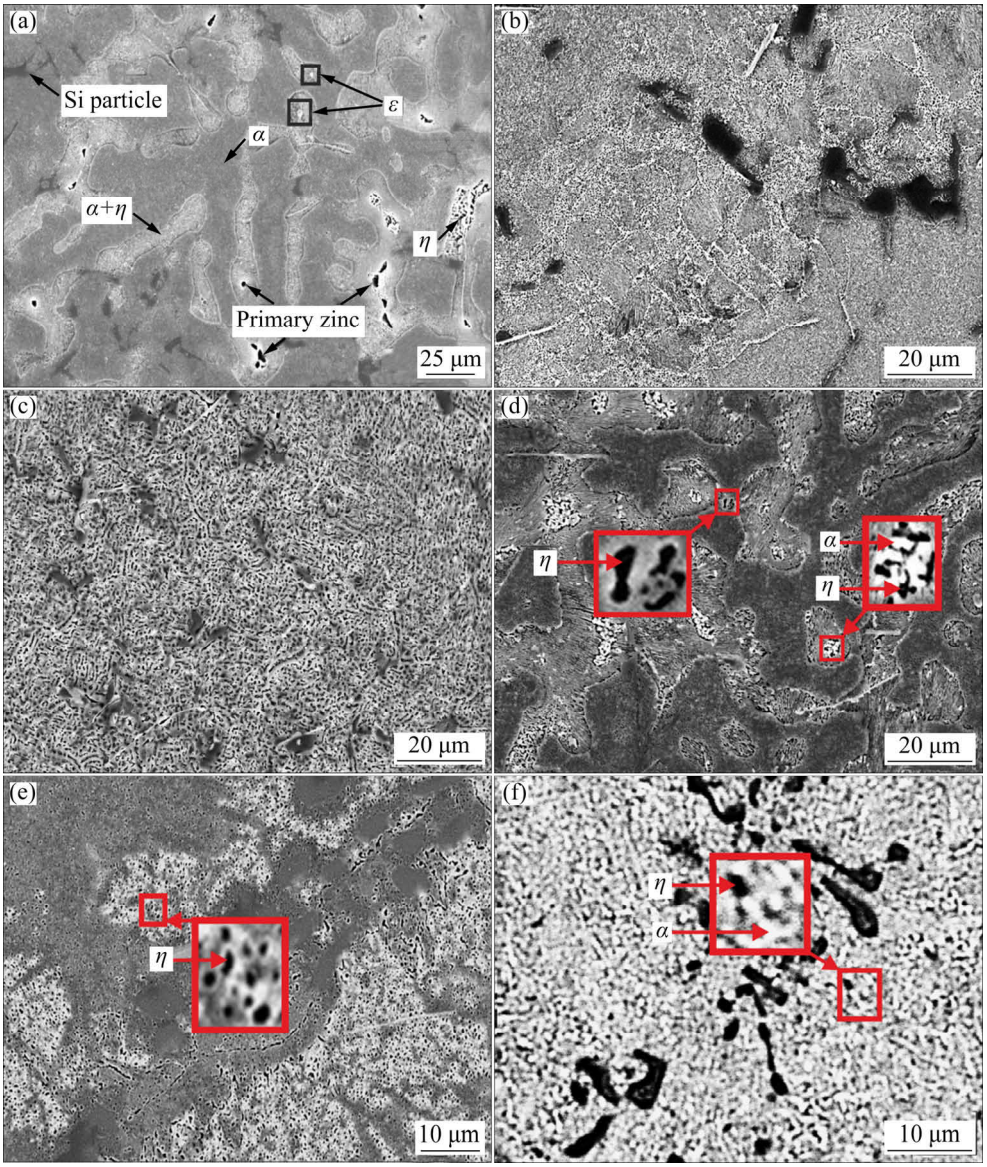

Fig. 3 SEM micrographs of as-cast (a), and H1 (b), H2 (c), T5 (d), T6 (e) and T7 (f) heat-treated microstructures of Zn−40Al−2Cu−2Si alloy

phases in the microstructure of the alloy samples. It can be seen that all the heat treatments, except T5 resulted in the removal of dendritic microstructure of the alloy. T5 heat treatment had no influence on the dendritic microstructure of the alloy, but resulted in the formation of zinc-rich fine precipitates as observed with the other heat treatments (Fig. 3(d)). It can also be seen that the microstructure of the T6 heat-treated sample of the alloy was not revealed well by chemical etching Fig. 3(e). This can be attributed to the effect of residual and coherency stresses that develop during quenching and aging of the sample. The microstructure of SAE 65 bronze consists of copper-rich α dendrites and eutectoid $\alpha+\delta$ phase mixture (Fig. 5).

3.2 Results of physical and mechanical tests

In order to determine the optimum aging time for T5, T6 and T7 heat treatments, hardness and length change of the alloy versus aging time curves were plotted, as shown in Figs. 6 and 7. The curves of Fig. 6 show that the changes in hardness and length of the alloy become almost stable after an

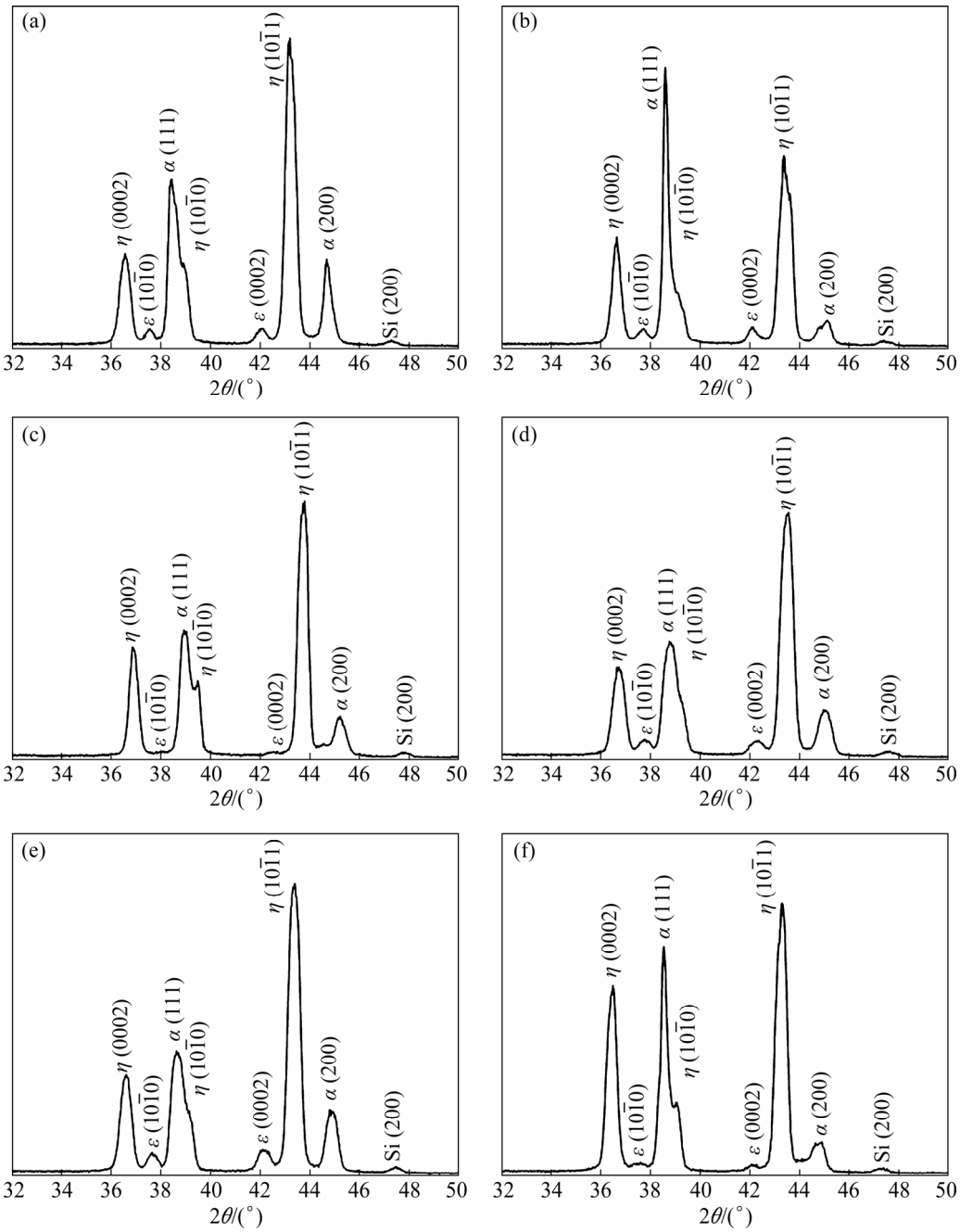

Fig. 4 XRD patterns showing phases in as-cast (a), and H1 (b), H2 (c), T5 (d), T6 (e) and T7 (f) heat-treated microstructures of Zn−40Al−2Cu−2Si alloy

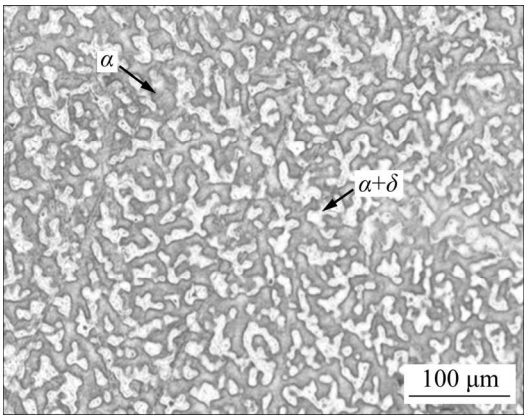

Fig. 5 SEM micrograph of microstructure of SAE 65 bronze

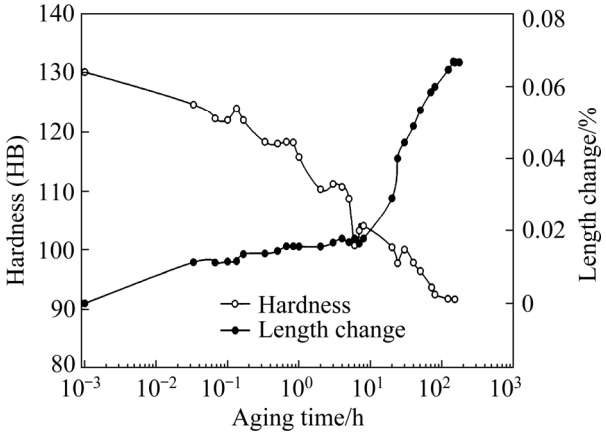

Fig. 6 Hardness and length change versus aging time curves of Zn−40Al−2Cu−2Si alloy obtained at 150 °C

aging time of approximately 100 h. Therefore, this period of time was considered to be a suitable aging time for the T5 heat treatment. After evaluation of the curves in Fig. 7, aging time periods of 2 min and 8 h at 180 °C are considered to be suitable for T6 and T7 heat treatments, respectively. This

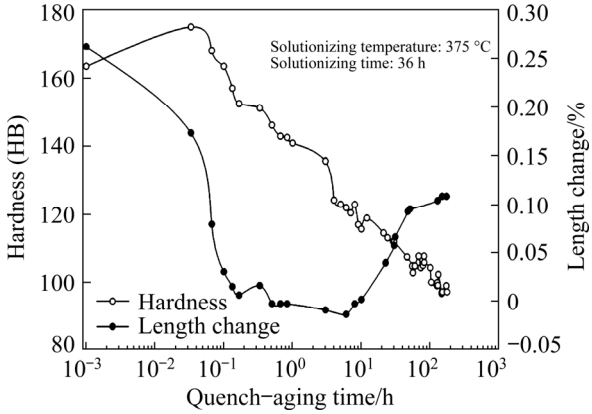

Fig. 7 Hardness and length change versus quench−aging time curves of Zn−40Al−2Cu−2Si alloy obtained at 180 °C

consideration was made according to the definition of these heat treatments [21].

The density, hardness, ultimate tensile strength, compressive strength, impact energy and elongation to fracture values of the as-cast and heat-treated samples of Zn−40Al−2Cu−2Si alloy and SAE 65 bronze are given in Table 3. It is shown that the hardness, tensile strength and compressive strength values of the alloy increased after H1 and T6 heat treatments. However, all the heat treatments, except T6 caused an increase in the elongation to fracture values of the alloy.

3.3 Results of friction and wear tests

Friction coefficient, temperature, wear volume and average surface roughness versus sliding distance curves of the as-cast and heat-treated samples of Zn−40Al−2Cu−2Si alloy and SAE 65 bronze are given in Figs. 8−11. The friction coefficient and temperature of the alloy samples

Table 3 Density, hardness, tensile strength, compressive strength and elongation to fracture values of as-cast and heat-treated samples of Zn−40Al−2Cu−2Si alloy and SAE 65 bronze

Material	Condition	Density/ ($kg·m^{-3}$)	Hardness (HB)	Tensile strength/MPa	Compressive strength/MPa	Elongation to fracture/%
Zn−40Al−2Cu−2Si alloy	As-cast	4219	126±3	375±6	909±12	1.4±0.4
	H1 treated	4217	139±2	401±8	962±19	1.8±0.5
	H2 treated	4212	104±3	301±5	811±17	2.0±0.6
	T5 heat-treated	4217	93±2	275±6	716±22	1.6±0.5
	T6 heat-treated	4188	174±2	475±10	1159±25	1.0±0.4
	T7 heat-treated	4219	123±3	331±6	828±23	1.5±0.6
SAE 65 bronze	As-cast	8770	105±4	286±5	1231±24	8.0±2.0

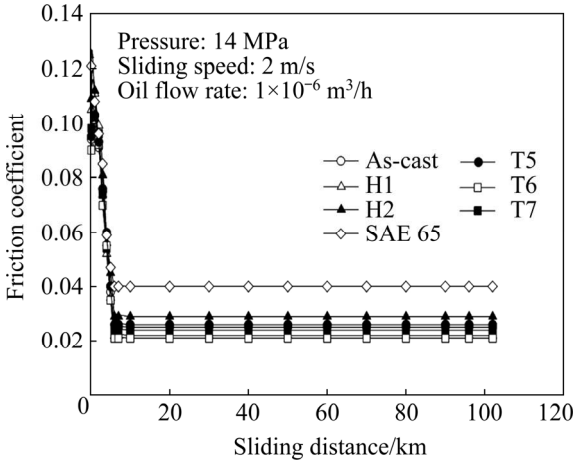

Fig. 8 Friction coefficient versus sliding distance curves of as-cast and heat-treated samples of Zn−40Al−2Cu−2Si alloy and SAE 65 bronze

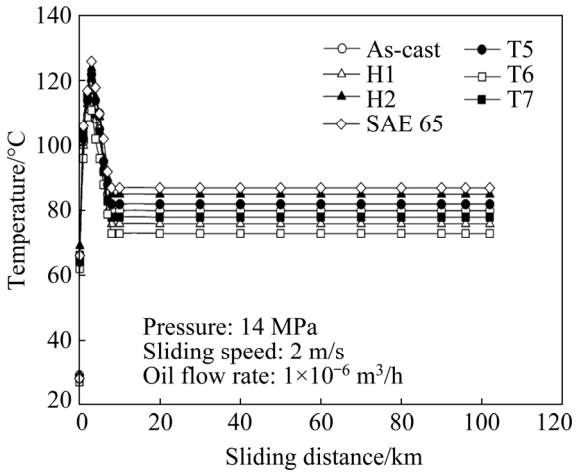

Fig. 9 Temperature versus sliding distance curves for as-cast and heat-treated samples of Zn−40Al−2Cu−2Si alloy and SAE 65 bronze

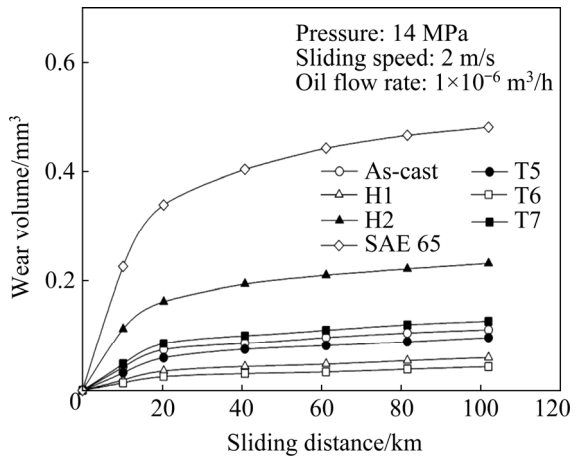

Fig. 10 Wear volume versus sliding distance curves for as-cast and heat-treated samples of Zn−40Al−2Cu−2Si alloy and SAE 65 bronze

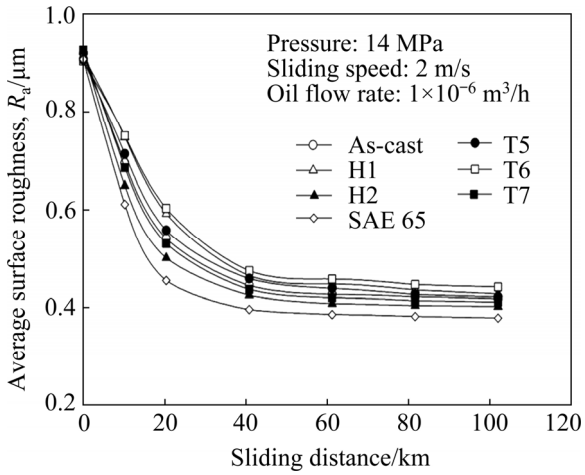

Fig. 11 Average surface roughness versus sliding distance curves for as-cast and heat-treated samples of Zn−40Al−2Cu−2Si alloy and SAE 65 bronze

reached constant levels after showing a sudden increase and a sharp decrease at the beginning of the wear tests (Figs. 8 and 9). The wear volume values of the samples increased rapidly at the initial period of the test run and reached steady state levels after a sliding distance of approximately 20 km (Fig. 10). The surface roughness values of the wear samples showed a sharp decrement and reached steady state levels after a sliding distance of about 40 km (Fig. 11).

The values of friction coefficient, temperature, wear volume and average surface roughness measured at the end of the tests are shown in Fig. 12. The measured friction coefficient and temperature values also correspond to the steady-state levels. It is shown that Zn−40Al−2Cu−2Si alloy exhibited the lowest friction coefficient, temperature and wear volume after T6 heat treatment. It can also be seen that the friction coefficient, temperature and wear volume values of the alloy decreased after H1 and T5 heat treatments, but increased by the application of H2 and T7 heat treatments. The highest and lowest values of the average surface roughness were obtained after T6 and H2 heat treatments, respectively.

SEM images of the wear surface of the as-cast and heat-treated samples of Zn−40Al−2Cu−2Si alloy and SAE 65 bronze are shown in Figs. 13 and 14. These micrographs show that the worn surfaces of the alloy samples were characterized by smearing of the adhered wear material and scratches. Scratches were more evident on the wear

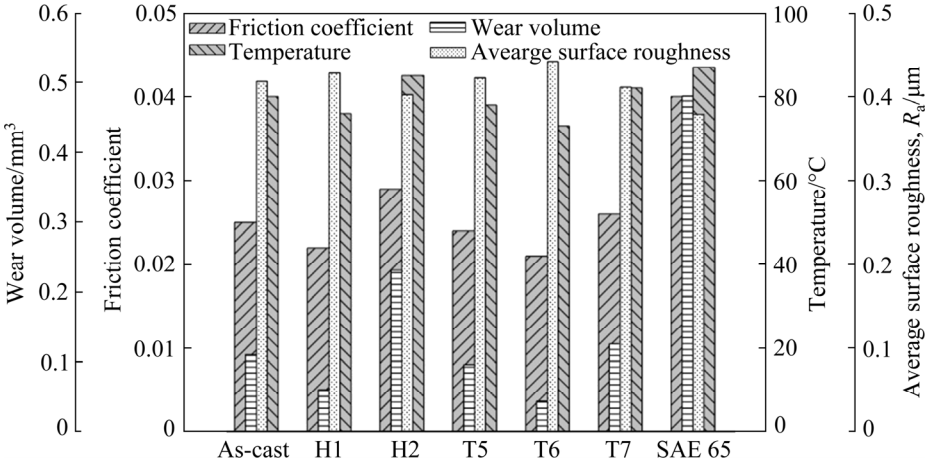

Fig. 12 Friction coefficient, temperature, wear volume and average surface roughness values obtained from as-cast and heat-treated samples of Zn−40Al−2Cu−2Si alloy and SAE 65 bronze at end of tests

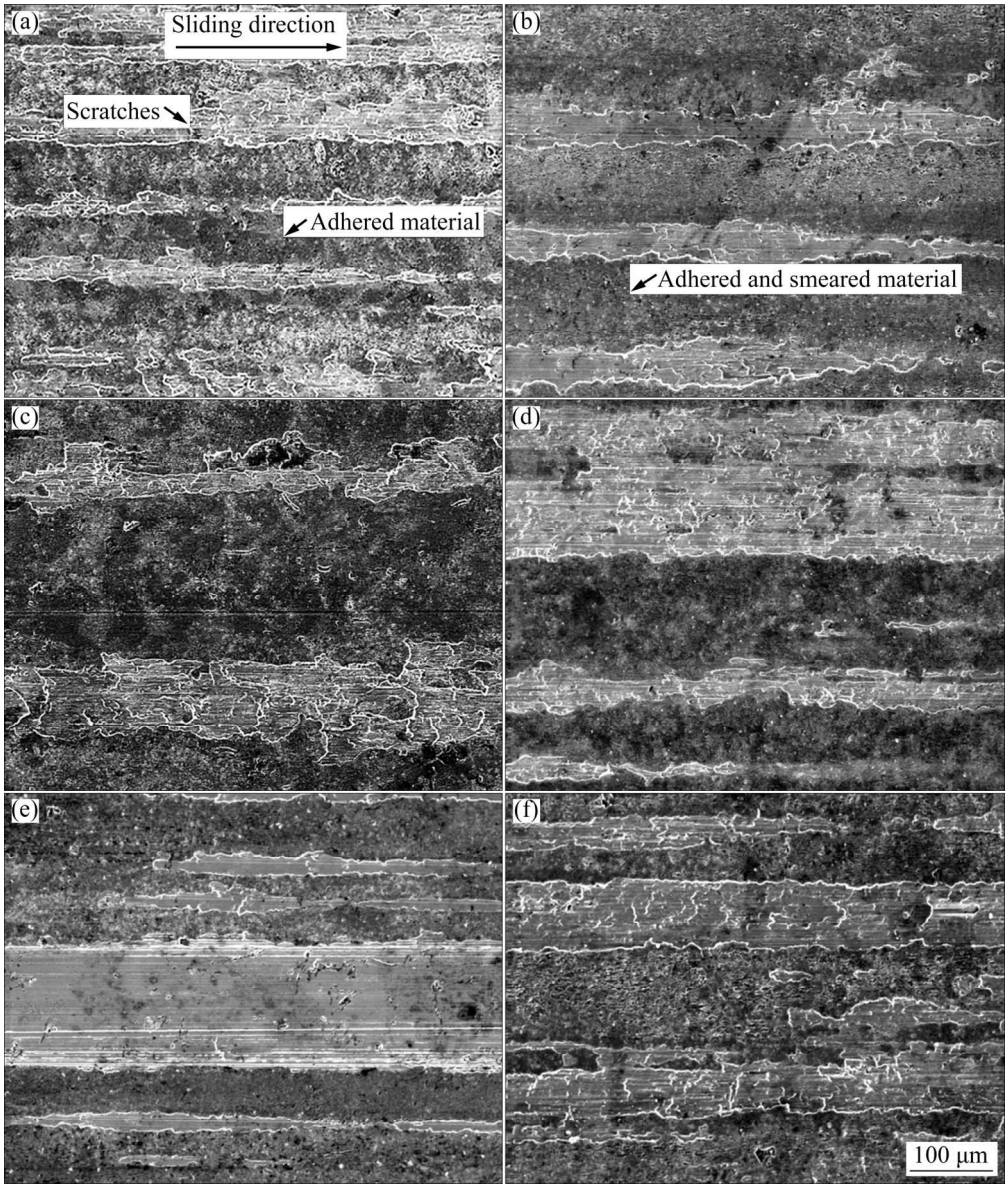

Fig. 13 SEM images of worn surface of as-cast (a), and H1 (b), H2 (c), T5 (d), T6 (e) and T7 (f) heat-treated samples of Zn−40Al−2Cu−2Si alloy

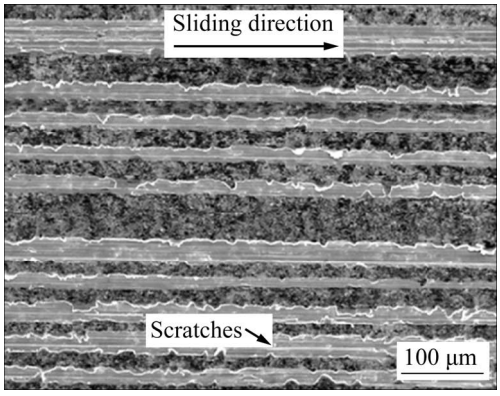

Fig. 14 SEM image of worn surface of SAE 65 bronze sample

surface of the T6 heat-treated sample of the alloy and SAE 65 bronze (Figs. 13(e) and 14). In addition, less smeared areas were observed on the worn surface of the bronze sample (Fig. 14).

Subsurface microstructural changes were observed in the as-cast and T6 heat-treated wear samples of Zn−40Al−2Cu−Si alloy (Figs. 15(a, e). These changes resulted in the formation of a coarser micro structured surface layer with a thickness varying from 2 to 5 μm. However, no distinct subsurface microstructural alterations were observed in the as-cast, H1, H2, T5 and T7 heat-treated samples of the alloy and the wear sample of the bronze (Figs. 15(b−f) and 16).

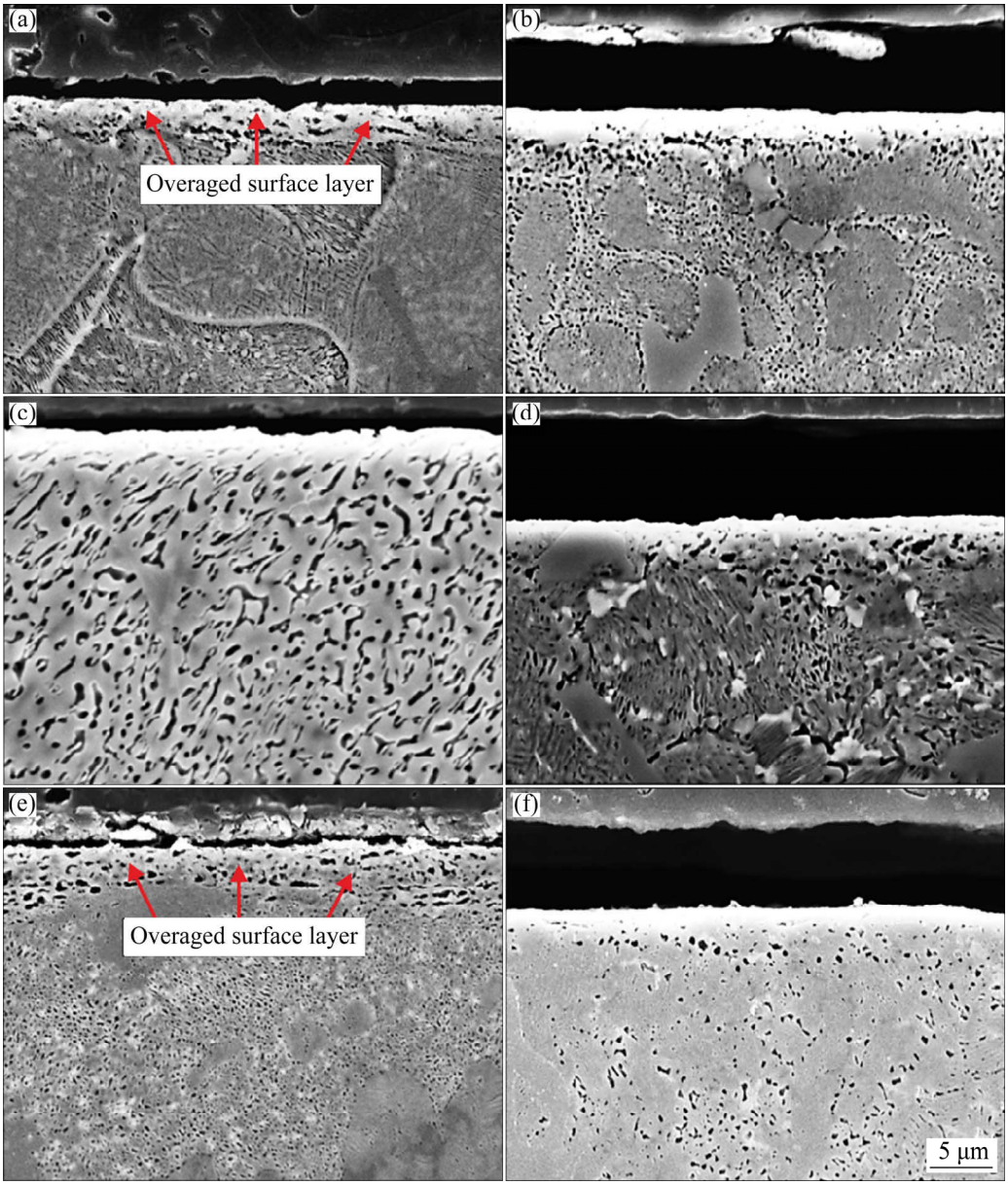

Fig. 15 Subsurface microstructures of as-cast (a), and H1 (b), H2 (c), T5 (d), T6 (e) and T7 (f) heat-treated wear samples of Zn−40Al−2Cu−2Si alloy

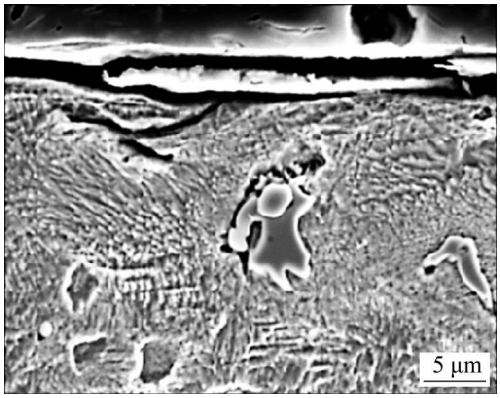

Fig. 16 Subsurface microstructure of wear sample of SAE 65 bronze

4 Discussion

The as-cast microstructure of Zn−40Al−2Cu−2Si alloy consisted of aluminum-rich α dendrites, eutectoid $\alpha+\eta$ and copper-rich ε ($CuZn_4$) phases, and silicon particles, as seen in Fig. 3(a). The explanation for the formation of this microstructure in this alloy was reported in the published works [9−11]. All the heat treatments, except T5 resulted in the removal of dendritic microstructure of the alloy and the formation of α grains and zinc-rich fine precipitates (Figs. 3(b−f)). These microstructural changes were attributed to the transformation of the supersaturated α/β solid solution into α and η phases by a eutectoid reaction that occurs during cooling or aging [22−25]. However, T5 heat treatment had no significant influence on the microstructure of the alloy (Fig. 3(d)). It is an expected result, since this heat treatment was carried out at a temperature well below the critical transformation temperature. During this treatment, only metastable phases of the as-cast microstructure of the alloy transform to stable ones. Since the volume fraction of such phases is very low, T5 heat treatment is not expected to cause significant changes in the microstructure of the alloy.

The hardness and strength of Zn−40Al−2Cu−2Si alloy decreased, but its elongation to fracture and impact energy increased after T5, T7 and H2 heat treatments (Table 3). The changes observed in the mechanical properties of this alloy, may be attributed to the removal of the residual stresses and decomposition of metastable phases of the as-cast microstructure during these heat treatments. However, these properties of the alloy showed opposite changes after T6 and H1 heat treatments (Table 3). The changes observed in the properties of the alloy after T6 and T7 heat treatments can be explained in terms of precipitation hardening. It is known that T6 heat treatment is an aging process, but T7 heat treatment involves overaging [21]. The hardness and strength of the supersaturated α solid solution increase, but its ductility decreases due to the distortion of the crystal lattice planes caused by coherency stresses developed during aging [26,27]. However, opposite changes take place during overaging period due to the loss of coherency or gradual decrease in the coherency stresses and grain growth [26,27].

The friction coefficient and the surface temperature of the alloy samples became almost constant at sliding distances of approximately 6 and 8 km, respectively, after showing a sudden increase and a rapid decrement at the initial stage of the test run (Figs. 8 and 9). Sharp increment in the friction coefficient and temperature of the samples at the beginning of the test can be attributed to the metal-to-metal contact, which takes place due to the inadequate oil film thickness on the mating surfaces [28,29]. When the oil film thickness becomes sufficient to separate the rubbing surfaces, friction coefficient becomes almost constant [30]. Since the temperature of the wear sample is directly proportional to the heat generated by friction, it follows the changes in the friction coefficient and becomes almost constant at a sliding distance of approximately 8 km (Fig. 8). The wear volume and the average surface roughness of the alloy samples reach steady states at a sliding distance of approximately 40 km after showing a sharp increase and a sudden decrease in the initial period of test run, respectively (Figs. 10 and 11). The increase in wear volume at the beginning of the test results from the metal-to-metal contact that occurs due to insufficient oil film thickness to separate the rubbing surfaces [30]. However, the decrease in average surface roughness may be attributed to the shearing of asperities during sliding with grinding and formation of a smooth layer on the sample and disk surfaces due to adhering and smearing of the wear material. It may be stated that when a smooth layer is formed on the rubbing surfaces the average surface roughness and wear volume of the alloy sample reach steady states.

The sample of the alloy subjected to T6 heat treatment exhibited the lowest friction coefficient, temperature and wear volume, but the highest surface roughness among all the samples (Fig. 12). H1 heat treatment also had similar effects on these values, but to a less extent. The decrement observed in the friction coefficient and wear volume of the alloy samples can be related to the increase in their hardness and strength after H1 and T6 heat treatments. As reported in the literatures, the friction coefficient and wear volume of the materials decrease as their hardness and strength increase [28,29,31]. Therefore, the coefficient of friction and wear volume of the alloy samples are expected to decrease with H1 and T6 heat treatments. The increase in the surface roughness may be related to the amount of wear material adhered to the rubbing surface of the samples. As the wear volume decreases, the amount of material adhered to the sample surface decreases. This means that less material is available for the formation of a smooth surface layer by smearing. In other words, the area of the smooth surface layer decreases with increasing wear resistance. This gives rise to a slightly higher average surface roughness compared to that obtained from the other wear samples.

The decrease observed in the friction coefficient and wear volume of the samples subjected to T5 heat treatment (Fig. 12) may be related to the precipitation of the zinc-rich particles and their role in the wear process. It is known that, the zinc-rich phase reduces the friction between the mating surfaces by facilitating the sliding [16,32]. In addition, adhesive wear becomes more effective for the alloy samples subjected to T5 heat treatment, because this heat treatment reduces the hardness and strength of the alloy, but increases its ductility (Table 3). This means that most of the wear material adheres to the sample surface and this reduces the amount of wear loss.

The observed increment in the wear volume of the alloy samples subjected to H2 and T7 heat treatments can be attributed to their effects on the microstructure and mechanical properties of the alloy. These heat treatments reduce the hardness and strength of the alloy by producing a coarser lamellar microstructure (Figs. 3(d, f). According to Archard's wear law, as the hardness and strength of the materials decrease, their wear volume increases [29]. Therefore, the wear volume of the alloy is expected to increase after H2 and T7 heat treatments.

Smeared material and scratches were observed to be the main features of the worn surface of the alloy samples (Figs. 13(a−f). It is known that smearing occurs by back transferring and adhering of the wear debris to the rubbing surfaces and the scratches are formed by the removal of hard silicon and probably small ε particles detached from the wear surface of the specimens, as reported in the previously published works [8,12−16]. Since smearing of the adhered material is taken as the indication of adhesive wear and scratches correspond to abrasive wear [33,34], these observations indicate that wear of the alloy and the bronze takes place by both adhesion and abrasion. However, the wear samples of the alloy showed larger smeared regions than the bronze samples (Figs. 13(a−f) and 14). Because of these observations, it may be stated that adhesion is the dominant wear mechanism for the alloy, but the abrasion is more effective in the wear of the bronze.

Subsurface microstructural changes were observed in the as-cast and T6 heat-treated wear samples of the alloy (Figs. 15(a, e)), but the H1, H2, T5 and T7 heat-treated samples and the bronze showed no distinct microstructural alterations (Figs. 15(c−f) and 15). These microstructural changes resulted in the formation of a surface layer with a coarser microstructure. The observed subsurface microstructural changes can be attributed to the transformation of the metastable phases and overaging of the surface material that takes place during the wear test due to frictional heat and applied pressure. Formation of surface layer with a coarser microstructure can promote adhesive wear of the alloy samples due to softening. These observations also indicate that the H1, H2, T5 and T7 heat-treated wear samples of the alloy and the bronze have relatively more stable microstructures with less amount of metastable phases.

5 Conclusions

(1) The as-cast microstructure of Zn−40Al−2Cu−2Si alloy consists of aluminum-rich α

dendrites, eutectoid α+η and copper-rich ε ($CuZn_4$) phases and silicon particles.

(2) H1, H2, T6 and T7 heat treatments remove dendritic microstructure of the Zn−40Al−2Cu−2Si alloy, but T5 heat treatment has no influence on the appearance of its microstructure.

(3) Hardness and strength of Zn−40Al−2Cu−2Si alloy increase by the application of H1 and T6 heat treatments while H1, H2, T5 and T7 heat treatments improve its elongation to fracture.

(4) H1, T5 and T6 heat treatments reduce the friction coefficient, temperature and wear volume of Zn−40Al−2Cu−2Si alloy. However, this alloy exhibits the lowest friction coefficient, working temperature and wear volume after T6 heat treatment. Therefore, T6 heat treatment appears to be the best process for the lubricated tribological applications of this alloy at a pressure of 14 MPa.

(5) An overaged surface layer with a coarser microstructure is formed in the as-cast and T6 heat-treated samples of Zn−40Al−2Cu−2Si alloy during lubricated bearing applications at a pressure of 14 MPa.

(6) Zn−40Al−2Cu−2Si alloy in both as-cast and heat-treated conditions exhibits lower wear volume or higher wear resistance than SAE 65 bronze. This indicates that this alloy can replace the bronze in bearing applications. It may also be concluded that the journal bearings manufactured from heat-treated Zn−40Al−2Cu−2Si alloy can be used successfully in diesel engines.

Acknowledgments

This work was supported by Scientific Research Projects Coordination Unit of Karadeniz Technical University, Turkey (No. 2008.112.03.1).

References

[1] GUTIÉRREZ-MENCHACA J, TORRES-TORRES D, GARAY-TAPIA A M. Microstructural, mechanical and thermodynamic study of the as-cast Zn−Al−Sr alloys at high Sr content [J]. Journal of Alloys and Compounds, 2020, 829: 154511.

[2] ZHANG Jian-jun, WANG Qing-zhou, JIAO Zhi-xian, CUI Chun-xiang, YIN Fu-xing, YAO Chang. Effects of combined use of inoculation and modification heat treatment on microstructure, damping and mechanical properties of Zn−Al eutectoid alloy [J]. Materials Science and Engineering A, 2020, 790: 139740.

[3] HEKİMOĞLU A P, SAVAŞKAN T. Lubricated wear characteristics of Zn−15Al−3Cu−1Si alloy and SAE 660 bronze [J]. Journal of the Faculty of Engineering and Architecture of Gazi University, 2018, 33: 145−154.

[4] YANG Yang, LIANG Lu-xin, WU Hong, LIU Bo-wei, FANG Qi-hong. Effect of zinc powder content on tribological behaviors of brake friction materials [J]. Transactions of Nonferrous Metals Society of China, 2020, 30: 3078−3092.

[5] SAVAŞKAN T, MALEKI R A. Friction and wear properties of Zn−25Al-based bearing alloys [J]. Tribology Transactions, 2014, 57: 435−444.

[6] SAVAŞKAN T, HEKİMOĞLU A P. Microstructure and mechanical properties of Zn−15Al-based ternary and quaternary alloys [J]. Materials Science and Engineering A, 2014, 603: 52−57.

[7] YAO Cai-zhen, TAY S L, ZHU Tian-ping, SHANG Hong-fei, GAO Wei. Effects of Mg content on microstructure and electrochemical properties of Zn−Al−Mg alloys [J]. Journal of Alloys and Compounds, 2015, 645: 131−136.

[8] SAVAŞKAN T, HEKİMOĞLU A P. Relationships between mechanical and tribological properties of Zn−15Al-based ternary and quaternary alloys [J]. International Journal of Materials Research, 2016, 107: 646−652.

[9] SAVAŞKAN T, AYDINER A. Effects of silicon content on the mechanical and tribological properties of monotectoid-based zinc–aluminium–silicon alloys [J]. Wear, 2004, 257: 377−388.

[10] SAVAŞKAN T, PÜRÇEK G, HEKİMOĞLU A P. Effect of copper content on the mechanical and tribological properties of ZnAl27-based alloys [J]. Tribology Letters, 2003, 15: 257−263.

[11] SAVAŞKAN T, HEKİMOĞLU A P, PÜRÇEK G. Effect of copper content on the mechanical and sliding wear properties of monotectoid-based zinc−aluminium−copper alloys [J]. Tribology International, 2004, 37: 45−50.

[12] SAVAŞKAN T, BİCAN O. Effects of silicon content on the microstructural features and mechanical and sliding wear properties of Zn−40Al−2Cu−(0−5)Si alloys [J]. Materials Science and Engineering A, 2005, 404: 259−269.

[13] SAVAŞKAN T, HEKİMOĞLU A P. Effect of quench–ageing treatment on the microstructure and properties of Zn−15Al−3Cu alloy [J]. International Journal of Materials Research, 2015, 106: 481−487.

[14] HEKİMOĞLU A P, ÇALIŞ M. Effects of titanium addition on structural, mechanical, tribological, and corrosion properties of Al−25Zn−3Cu and Al−25Zn−3Cu−3Si alloys [J]. Transactions of Nonferrous Metals Society of China, 2020, 30: 303−317.

[15] BİCAN O, SAVAŞKAN T. Influence of T5 heat treatment on the microstructure and lubricated wear behavior of ternary ZnAl40Cu2 and quaternary ZnAl40Cu2Si2.5 alloys [J]. Materialwissenschaft und Werkstofftechnik, 2020, 51: 383−390.

[16] SAVAŞKAN T, BİCAN O. Dry sliding friction and wear properties of Al−25Zn−3Cu−(0−5)Si alloys in the as-cast and heat-treated conditions [J]. Tribology Letters, 2010, 40: 327−336.

[17] PENG Ying-hao, LIU Chong-yu, WEI Li-li, JIANG Hong-jie, GE Zhen-jiang. Quench sensitivity and microstructures of high-Zn-content Al−Zn−Mg−Cu alloys with different Cu contents and Sc addition [J]. Transactions of Nonferrous

Metals Society of China, 2021, 31: 24−35.
[18] KAUFMAN J G. Introduction to aluminum alloys and tempers [M]. USA: ASM International, 2000.
[19] TOTTEN G E. ASM handbook. Heat treating of nonferrous alloys [M]. Volume 4E. USA: ASM International, 2016.
[20] HEYWOOD J B. Internal combustion engine fundamentals [M]. New York: McGraw Hill Book Company, 1988.
[21] EN 1706. Aluminium and aluminium alloys−Castings−Chemical composition and mechanical properties [S]. 2010.
[22] LEE PEKWAH PEARL, SAVAŞKAN T, LAUFER E. Wear resistance and microstructure of Zn−Al−Si and Zn−Al−Cu alloys [J]. Wear, 1987, 117: 79−89.
[23] SAVAŞKAN T, MURPHY S. Decomposition of Zn−Al alloys on quench–aging [J]. Materials Science and Technology, 1990, 6: 695−704.
[24] MURPHY S. Solid-phase reactions in the low-copper part of the Al−Cu−Zn system [J]. Materials Science, 1980, 71: 96−102.
[25] MURPHY S. The structure of the *T′* phase in the system Al−Cu−Zn [J]. Metal Science, 1975, 9: 163−168.
[26] ABBASCHIAN R, ABBASCHIAN L. REED-HILL R E. Physical metallurgy principles [M]. 4th ed. Stanford: Cengage Learning, 2008.
[27] AVNER S H. Introduction to physical metallurgy [M]. India: McGraw Hill, 1997.
[28] HALLING J. Principles of tribology [M]. London: Macmillan Education Ltd, 1989.
[29] HUTCHINGS I M. Tribology: Friction and wear of engineering materials [M]. Great Britain: Edward Arnold Publishers Ltd, 1992.
[30] SAVAŞKAN T, TAN H O, MALEKI R A. Effects of contact pressure and sliding distance on the lubricated friction and wear properties of Zn−25Al−3Cu alloy: A comparative study with SAE 65 bronze [J]. International Journal of Materials Research, 2015, 106: 1060−1066.
[31] HUTCHINGS I M. Tribology: Principles and design applications [J]. Tribology International, 1992, 25: 217−218.
[32] PRASAD B K. Sliding wear response of a zinc-based alloy and its composite and comparison with a gray cast iron: Influence of external lubrication and microstructural features [J]. Materials Science and Engineering A, 2005, 392: 427−439.
[33] HEKİMOĞLU A P, SAVAŞKAN T. Effects of contact pressure and sliding speed on the unlubricated friction and wear properties of Zn−15Al−3Cu−1Si alloy [J]. Tribology Transactions, 2016, 59: 1114−1121.
[34] BHUSHAN B. Modern tribology handbook [M]. CRC Press, 2001.

热处理对 Zn−40Al−2Cu−2Si 合金力学性能和磨损性能的影响

Temel SAVAŞKAN[1], Zeki AZAKLI[2], Ali Paşa HEKIMOĞLU[3]

1. Mechanical Engineering Department, Haliç University, 34445, İstanbul, Turkey;
2. Mechanical Engineering Department, Gümüşhane University, 29010, Gümüşhane, Turkey;
3. Mechanical Engineering Department, Recep Tayyip Erdogan University, 53100, Rize, Turkey

摘　要：为了研究热处理对 Zn−40Al−2Cu−2Si 合金力学性能和磨损性能的影响，采用不同工艺对其进行热处理，包括均匀化后空冷(H1)、均匀化后炉冷(H2)、稳定化(T5)和淬火−时效(T6 和 T7)。通过金相、力学实验和磨损实验，研究不同热处理工艺对该合金力学性能和摩擦学性能的影响，并于 SAE 65 青铜进行对比。磨损实验使用环块式实验装置。结果表明，采用 H1 和 T6 热处理可提高合金的硬度、抗拉强度和抗压强度，除 T6 热处理外的其他热处理均可提高合金的断裂伸长率。经 H1、T5 和 T6 热处理后，合金的摩擦因数和磨损量减小，其中 T6 热处理后合金的摩擦因数和磨损量最低。因此，T6 热处理为该合金应用于 14 MPa 压力下润滑摩擦的最佳工艺。与青铜相比，铸态和热处理态的 Zn−40Al−2Cu−2Si 合金磨损量较低、耐磨性较高。

关键词：Zn−Al 基合金；热处理；结构特征；力学性能；润滑摩擦磨损

(Edited by Bing YANG)